CW emission and self-pulsing in III/V SiN hybrid laser with narrowband mirror

Cristina Rimoldi[1], Lorenzo Columbo[1], Sebastian Romero-García[2], Jock Bovington[3] and Mariangela Gioannini[1]

[1]Dipartimento di Elettronica e Telecomunicazioni, Politecnico di Torino, Corso Duca degli Abruzzi 24, Torino, IT-10129, Italy
[2]CISCO Optical, Nuremberg, Germany
[3]CISCO Systems, San José, CA, USA
*cristina.rimoldi@polito.it

We investigate the CW stability of a III-V SiN hybrid laser. By detuning the lasing frequency with respect to the narrowband mirror reflectivity peak, we observe regimes of ultra-damped relaxation oscillations, turbulence, and self-pulsing, caused by the interplay of four-wave mixing, the non-null linewidth enhancement factor, and the narrowband reflectivity. The laser tolerance to optical feedback is also investigated, for the purpose of providing indications on isolator-free operation.
Keywords: *Silicon photonics, hybrid lasers, optical feedback, self-pulsing*

INTRODUCTION

Laser sources integrated in Silicon Photonic (SiPh) platforms are essential for the realization of low-cost optical transmitters for optical interconnects, for sensing and LIDAR applications. These lasers usually consist of a III-V gain material for light generation and amplification coupled to the rest of the silicon photonic chip, providing the laser mirror facet and extending the laser cavity. The design of the SiPh mirror can include several components, such as micro-rings, delay lines, Mach-Zehnder interferometers, and DBR reflectors, all providing very narrow band (a few GHz bandwidth) dispersive reflectors [1], which allow to obtain long external cavity narrow linewidth lasers with wide tunability [2,3]. While much effort has been dedicated to the experimental and theoretical study of the laser linewidth reduction, few works have been focused on the study of other dynamical characteristics. Alongside narrow linewidth and CW emission, generation of self-pulsing and chaotic regimes was also reported [2,3]. In this work, we theoretically investigate the impact of the dispersive narrow band reflector in the dynamical performance of the laser. First, we consider the dynamics of the solitary laser and we analyze when and why CW emission can turn into a multimode regime. We demonstrate that several dynamical regimes can be observed, ranging from CW ultra-stable (where the laser relaxation oscillations are strongly damped) to self-pulsing or turbulent. These regimes have been experimentally observed [2,3] via the tuning of the lasing frequency, however they lack, to the best of our knowledge, a theoretical description able to explain the reasons behind their occurrence. Our work proves that these regimes are due to the interplay between the non-null linewidth enhancement factor and four-wave mixing in the reflective semiconductor optical amplifier and depend on the narrow bandwidth of the SiPh mirror and on the laser effective length. In the second part we discuss how the external optical feedback (due to spurious back-reflections coming from the other components of the SiPh circuit or from the output optical fiber) destabilize the CW emission. In the framework of investigating laser design for isolator-free operation [4,5], we study the laser tolerance to optical feedback and we highlight regions of ultra-stability, with tolerance to optical feedback up to -10 dB. The presented work provides a versatile tool for the analysis of external cavity hybrid lasers and our results can potentially be extended to other laser configurations.

METHODS

We consider the hybrid laser illustrated in Fig 1(a). This laser consists of an off-the-shelf III-V MQW 1mm long HR/AR RSOA edge-coupled to a silicon photonic circuit based on two coupled Si_3N_4 micro-rings, which provide narrowband dispersive reflectivity through Vernier effect. The ring radii are chosen in order to maximize the tuning range and minimize the overlap of the ring resonance peaks near the lasing one. The ring coupling coefficients are chosen as equal to obtain maximum mirror reflectivity in the critical coupling regime. This configuration has been analyzed in [5]. The overall effective reflectivity of the SiPh mirror ($|r_R(\nu)|^2$ in Fig.1(a)) has an FWHM bandwidth of 6 GHz (unless otherwise specified), obtained through ring design. The peak of $|r_R(\nu)|^2$ is 3% and the output power is collected through the output coupler $T_{c,out}$=73% [5]. Detuning of the lasing frequency with respect to the effective reflectivity peak is obtained via tuning of the phase $\Delta\phi$ of the control section PS. To account for spurious optical back-reflection, we include the possibility of an external reflector (r_{ext}) at a distance L_{ext} from the output coupler; based on the origin of the back reflection, we assume that the external optical feedback can range from -40 dB to -10 dB and L_{ext} can vary from a few millimeters to a few centimeters. The numerical model applied in our analysis

is based on [6] and consists in a set of time-delayed algebraic differential equations at the reference plane of the AR-coated facet of the RSOA. The model accounts for the frequency-selective mirror and assumes a Lorentzian response for the rings around the reference frequency. In particular, an integral equation for propagation of the optical electric field in the RSOA is coupled to the delayed differential equations accounting for the response of the rings and to the rate equation for the average carrier density of the RSOA. A linear stability analysis (LSA) of the CW solutions of the laser [6] allows to address the impact of the dispersive mirror bandwidth, the tuning of the phase control section, and the external cavity on the laser dynamics. In particular, the main complex roots of the determinant of the linearized system for the CW perturbations result associated to the relaxation oscillation resonance (RO) and the photon-photon resonance (PPR) and give the frequency (real part of the roots, f_{pert}) and damping (imaginary part of the roots, γ_{pert}) of these resonances. Numerical simulations of the dynamical equations give the temporal evolution of the laser in terms of output power versus time, RIN spectra, integrated RIN, and optical spectra.

RESULTS AND DISCUSSION

In Fig. 1(b) we show the map of the integrated RIN (over a bandwidth of 25 GHz) computed for different values of RSOA bias current and detuning $\Delta\nu$ of the lasing frequency with respect to the effective reflectivity $|r_R(\nu)|$ peak. The blue region of low RIN (<-160 dBc/Hz) corresponds to a stable single-mode regime, while the red region of high RIN (>-130 dBc/Hz) corresponds to a multimode regime (which we will characterize as self-pulsing or turbulent in the following). The white dashed line is obtained through LSA and highlights the border beyond which single mode emission becomes unstable (i.e., when the imaginary part of the RO root becomes negative, leading to undamped RO).

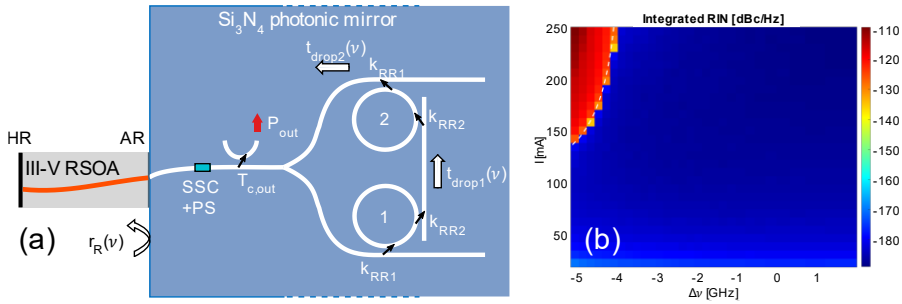

Fig. 1. Schematics of the III-V/SiN hybrid laser (a) and integrated RIN for different detuning $\boldsymbol{\Delta\nu}$ *of lasing frequency and RSOA bias current (b).* $\boldsymbol{\Delta\nu}$*=0 corresponds to lasing at the reflectivity peak which is centered at 1310 nm.*

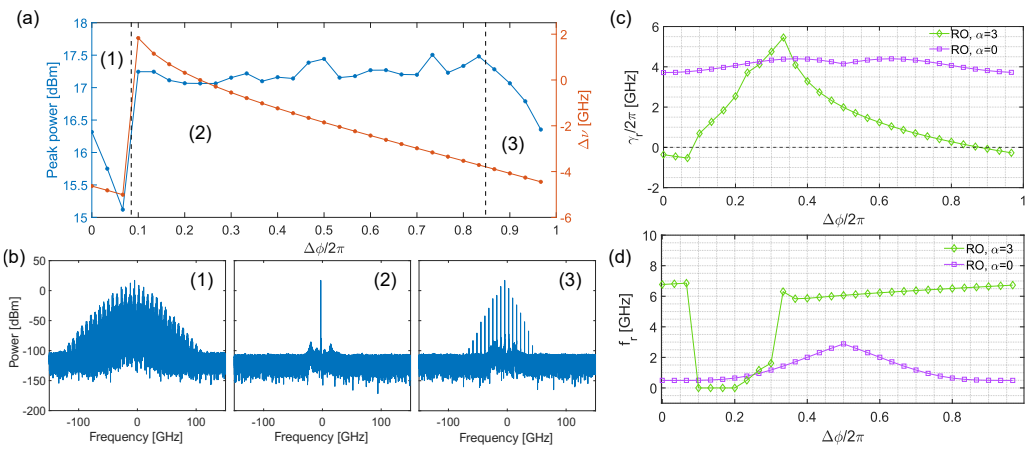

Fig. 2. Simulated lasing frequency and output power obtained through tuning of the phase section PS (a), optical spectra for the three dynamics regimes (b), damping (c) and frequency (d) of the roots associated to ROs for varying $\boldsymbol{\Delta\phi}$*. The RSOA bias current is fixed at 230 mA.*

Figure 2(a) shows the lasing frequency (in orange) and the average output power (in blue) for varying $\Delta\phi$ and fixed RSOA bias current of 230 mA. In Fig. 2(b) we report the optical spectra related to region 1 (turbulent regime), region 2 (stable single-mode emission), and region 3 (self-pulsing regime). In order to interpret the transition between single mode and multimode regimes, we consider the results of LSA, reported in Fig. 2(c,d), where we show, in green, the frequency (c) and damping rate (d) of the roots associated to ROs for different $\Delta\phi$: when the perturbation frequency becomes resonant with the beating between neighboring longitudinal modes, the damping becomes negative and we enter a CW unstable regime, characterized by undamped relaxation oscillations and consequent

multimode regime. In particular, for negative detuning of the lasing frequency $\Delta\nu$, the phase noise, caused by spontaneous emission and the α-parameter, turns into intensity noise due to the narrow band reflector and may cause another longitudinal mode to reach the lasing threshold. When the beating frequency between the competing modes is resonant with the RO, the latter becomes undamped and the laser typically enters in a self-pulsing regime. This effect tends to decrease for smaller (but still negative) detuning because of the contrasting effect of detuned loading [7], until an optimal maximum RO damping point is reached. The following reduction of the damping through further increase of $\Delta\phi$ is then due to the progressive reduction of the detuned loading effect. Note that, when the effect of the linewidth enhancement factor is neglected (purple curves in Fig. 2 (c,d)), this scenario is completely altered because of the reduced phase noise effect and self-pulsing and turbulent regimes are unachievable. The results in Fig. 2 are in accordance with experimental findings in [2,3] and can exemplify a valuable approach to interpret experimental results. As a general trend, we show in Fig. 3(a) that through proper design of effective mirror, narrow bandwidths can give higher damping factors in comparison with the case of a broad band reflector. The longer cavity effective length implies the emergence of a second peak in the IM response, associated to PPR, which plays an important role in the laser tolerance to optical feedback.

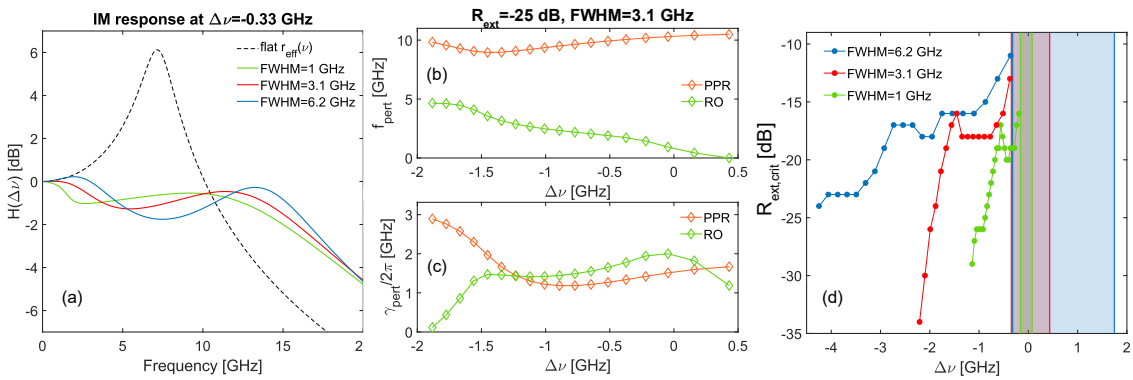

Fig. 3. Intensity-Modulation response for different reflectivity FWHMs at the RSOA bias current of 104 mA, corresponding to a power output of 20 mW (a), frequency (b) and damping (c) of the main roots for FWHM=3.1 GHz and R_{ext}=-25 dB versus detuning $\boldsymbol{\Delta\nu}$, and (d) critical feedback level versus detuning $\boldsymbol{\Delta\nu}$.

To study the effect of spurious back-reflections, we place e.g. the external reflector at L_{ext}=0.5 cm from the output coupler in Fig. 1(a). In Fig. 3(b,c), we show (for the case of FHWM=3.1 GHz and $r_{ext}^2 = R_{ext}$ =-25 dB) the main roots of the perturbations as a function of the detuning $\Delta\nu$, associated to RO (in green) and PPR (in orange). Here, while the laser is still stable, PPR has become less damped in comparison to ROs and will eventually trigger instability. This is shown in Fig. 3(d), where we report the critical feedback level (i.e., the value of R_{ext} for which the laser becomes CW unstable) as a function of the detuning for the three FWHMs. The shaded areas of matching colors identify regions of ultra-stability, where the laser is particularly resilient to optical feedback up to R_{ext}=-10 dB. In all cases, near the ultra-stable region, instability is triggered by PPR: smaller FSR for narrow mirror bandwidth favor longitudinal mode coupling and this leads to a lower tolerance to optical feedback, an effect that is not possible to capture through a standard single-mode Lang-Kobayashi approach [5].

In conclusion, while narrow mirror bandwidths are effective in suppressing ROs, the emergence of a second resonance due to PPR is not to be neglected and leads to lower laser feedback tolerance. Consequently, proper design of the SiPh mirror is necessary to guarantee the laser feedback tolerance while reducing the mirror bandwidth, which is important in light of enabling isolator-free operation.

References

[1] C. Xiang et al., *Widely tunable Si3N4 triple-ring and quad-ring resonator laser reflectors and filters*, 2018 IEEE 15th International Conference on Group IV Photonics (GFP), pp. 1–2 2018.

[2] D. Huang et al., *High-power sub-kHz linewidth lasers fully integrated on silicon,* Optica, vol. 6, pp. 745-752, 2019

[3] J. Mak et al., *Linewidth narrowing via low-loss dielectric waveguide feedback circuits in hybrid integrated frequency comb lasers*, Opt. Express, vol. 27, pp. 13307-13318, 2019

[4] Z. Zhang et al., *Linewidth enhancement factor in InAs/GaAs quantum dot lasers and its implication in isolator-free and narrow linewidth applications*, IEEE J. Sel. Top. Quantum Electron. Vol. 25, pp. 1–9, 2019.

[5] L. Columbo et al., *Efficient and optical feedback tolerant hybrid laser design for silicon photonics applications*, IEEE J. Sel. Top. Quantum Electron., vol. 26, pp. 1-10, 2020

[6] E. Detoma, *The complex way to laser diode spectra: example of an external cavity laser with strong optical feedback*, IEEE J. Quantum Electron., vol. 41, pp. 171-182, 2005.

[7] M. A. Tran et al., *Tutorial on narrow linewidth tunable semiconductor lasers using Si/III-V heterogeneous integration*, APL Photonics, vol. 4, pp. 111101, 2019.